Corrosion Detection in Steel Reinforced Aluminium Conductor Cables

Nisar Ali Jaffrey, Sujeewa Hettiwatte
School of Engineering and Information Technology
Murdoch University
Perth, Australia
n.jaffrey@live.com.au, s.hettiwatte@murdoch.edu.au

***Abstract*—Aluminum Conductor Steel Reinforced (ACSR) cables, as part of transmission lines, are used in severe environments in coastal areas and industrial zones for many years. These cables are affected by galvanic corrosion in the interface between the aluminum and steel strands. This paper investigates the existing methods of corrosion detection used in ACSR cables of overhead transmission lines, and estimates the location of corrosion through simulation in a computer program. The paper also analyses two promising methods of corrosion detection, namely "electromagnetic induction" and "time domain reflectometry (TDR)", and explains in detail their principle of operation and efficiency. The paper then thoroughly investigates the time domain reflectometry techniques by implementing it in a computer program, and the simulation results are discussed.**

***Index Terms*—ACSR; corrosion detection; electromagnetic induction; non-destructive testing; TDR**

I. Introduction

Overhead power transmission lines usually run in severe environments for many years and therefore the cables are exposed to harsh climatic variations such as wind, rain, pollution, etc. This leads to gradual degradation of the conductor and consequently to unexpected costly problems and poor power supply quality, if not dealt with in a timely fashion [1].

Aluminum conductor steel reinforced (ACSR) cables are the most commonly used conductors in overhead transmission lines. They are usually affected by galvanic corrosion, which is a key factor causing failure of the cable, and hence, refurbishment of the transmission line. A critical phase in this process is the loss of zinc from the galvanised steel strands because once the galvanising is lost the aluminum strands get exposed to rapid galvanic corrosion.

ACSR cables comprise a solid or stranded steel core surrounded by one or more layers of aluminum wires. So far, the majority of these conductors have lasted 25-40 years and in some cases up to 50 years [2], [3]. Therefore, long term exposure to severe environments means they require maintenance or refurbishment.

In power transmission system the common failure mechanism limiting the life of ACSR cable is internal corrosion [4]. In ACSR cables the chance of galvanic corrosion between the steel core and the aluminum strands has been, since the beginning, understood and preventive methods such as coating of steel strands applied. Nevertheless, certain atmospheric factors such as industrial pollution or marine salts in the air may still cause serious corrosion [5].

The main purpose of this paper is to evaluate the existing methods of corrosion detection used in ACSR cables, and to estimate the location of corrosion through simulation of a corroded cable in a computer program such as MATLAB.

II. Inspection Techniques

Non-destructive testing (NDT) is a technique in material science that conducts testing and scrutinising objects without causing any destruction to them. In electrical engineering, NDT has been used for detection, characterisation, localisation and sizing of discontinuities [2]. A number of NDT techniques have been introduced to detect and locate flaws in power transmission lines using various methods such as visual inspection, infrared camera inspection, ultrasonic inspection, neutron radiography, magnetic method, electromagnetic induction (eddy current), and time domain reflectometry

It is worth mentioning that the majority of these methods need mobilisation by foot, ground vehicle, or air vehicle, and require labour presence in the locality of the line. Traditionally, the most commonly used technique of fault detection has been the visual inspection method [6]. However, it cannot be used to detect internal corrosion in conductors. Helicopter carried infrared sensors can be used to investigate aluminum corrosion in transmission lines with severe deterioration and extremely corroded strands but is not suitable for early damage detection [7].

A. *Electromagnetic Induction Method (Eddy Current Testing)*

Electromagnetic induction is the physical basis for all eddy current NDT techniques. This technique can be used for detection of zinc loss from the steel strands inside ACSR [4]. Detectors based on this principle can identify any flaws in a conductor well before other non-destructive tests can do.

When an alternating current flows in a coil near a conductor, the magnetic field of the coil induces eddy currents in the conductor. These eddy currents control the loading on the coil and consequently the impedance on it. If there is a flaw on the conductor's surface beneath the coil, it will decrease the flow of eddy currents, which reduces the loading on the coil and increases the impedance on it. This is the basic concept for eddy current inspection [8].

Consider a pair of probe coils forming the sensing head as shown in Fig. 1, with one of the coils acting as field winding while the other as pick-up coil. The sensing head is designed to traverse along the wire.

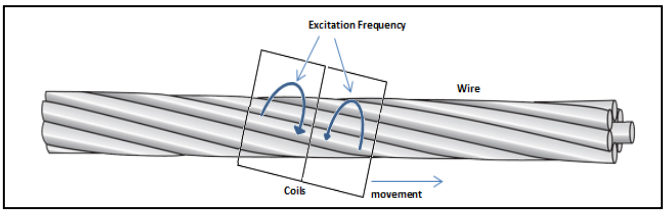

Figure 1. Principle of operation of eddy current testing method [9]

High frequency currents are passed through field windings and generate a magnetic field H that enter the conductor and induce eddy currents around each of the strands in the wire. These eddy currents produce alternating flux whose magnitude and phase are sensitive to any corrosion of the strands [4].

When the coils are traversed along a normal segment of the wire, the eddy currents in the wire induce some electromotive force in the coils with some particular impedance. On the contrary, when the coils are traversed over a corroded segment, the conductor induces a changed electromotive force on the coils, and the coils exhibit a change in the impedance. Thus, an uneven voltage is spotted on the pick-up coil. The detected voltage then undergoes numerous signal processing phases like amplification and phase detection to be further evaluated [9],[4]. This is the basic principle of eddy current testing.

Reference [4] identifies two component voltages namely "in-phase" and "quadrature" gained as output in this process. The in-phase voltage is only associated with aluminum strands while the steel strands are responsible for both in-phase and quadrature voltages.

The eddy currents induced around the strand constrain the flow of magnetic flux into the centre of the strand, and particularly at high frequencies this flux would be totally excluded from the whole strand cross-section [4].

The magnetic flux density B is given by:

$$B = \mu_0 H = \mu_0 H_0 \sin(\omega t) \quad (1)$$

Where μ_0 is the permeability of free space. Let R be the radius of both the field winding and the pick-up coil, and r be the radius of the strand. The voltage induced in the coil is given by:

$$V = -\frac{d\Phi}{dt} \quad (2)$$

$$V = -\mu_0 H_0 \ \omega \cos \omega t \ (\pi R^2 - \pi r^2) \quad (3)$$

In (3), part of the induced voltage, $-\mu_0 H_0 \ \omega \cos \omega t (\pi R^2)$, is not what we are looking for because it is associated with R, the radius of the coils, and can be removed by introducing an identical "compensation" voltage, V_C, in the opposite direction [4]. Hence, the resultant voltage is:

$$V_m = V - V_C \quad (4)$$

$$V_m = -\mu_0 H_0 \ \omega \cos \omega t \ (\pi r^2) \quad (5)$$

This voltage is proportional to the area of the strand, i.e. $V_m \alpha \pi r^2$. Equation (5) is applicable at very high frequencies only. If a detector is designed to operate at lower or intermediate frequencies then the penetration of flux into the strands needs to be considered. The penetration distance (skin depth) is given by [4]:

$$\delta = \sqrt{\frac{\rho}{\mu \pi f}} = \sqrt{\frac{2\rho}{\mu_r \mu_0 \omega}} \quad (6)$$

Where, ρ is the electrical resistivity and μ_r is the relative magnetic permeability of the strand. It can also be shown that for $\delta << r$, the flux $_p$ penetrating into the strand is given by:

$$\Phi_P = \pi r \mu_0 \mu_r \delta H_0 (\sin \omega t + \cos \omega t) \quad (7)$$

This flux possesses two equal components; one in phase with the applied field, $H_0 \sin \omega t$, the other in phase quadrature. This flux induces a voltage $\frac{d_p}{dt}$ in the pick-up coil besides that due to flux exclusion, given in (5). The total voltage is [4]:

$$\frac{d_p}{dt} = \pi \ r \ \mu_0 \ \mu_r \ \delta \ H_0 \ (w \cos \omega t - w \sin \omega t) \quad (8)$$

$$V_P = w \ \pi \ r \ \mu_0 \ \mu_r \ \delta \ H_0 \ (\sin \omega t - \cos \omega t)$$

$$\Phi_P = -\mu_0 \omega H_0 \pi r^2 \left[\left(1 - \frac{\delta \mu_r}{r}\right) \cos \omega t \left(\frac{\delta \mu_r}{r}\right) \sin \omega t\right] (9)$$

Equation (9) reduces to (5) at high frequencies.

The feasibility study on different detection methods by [9] suggests that the eddy current induction method is highly feasible for flaw detection, and finds that the method offers high sensitivity with outstanding practicality. Their findings are summarised in Table I [9].

TABLE I. COMPARISON OF VARIOUS TYPES OF NDT TECHNIQUES

Technique	Sensitivity	Ease of use	Applicable
Electromagnetic Induction	o	o	o
Magnetic Flaw Detection	o	×	×
Ultrasonic Method	^	×	×
Longitudinal Vibration	×	^	^
Bending Stiffness	×	o	^
Shooting Camera (visual)	^	^	^
Legend	***Excellent:*** *o*	***Fair:*** ^	***Poor:*** ×

a) Available Eddy Current Technology Detectors

A number of detectors based on this technology have been developed and commercialized. Some of the most popular ones around the world are discussed below.

1) Cormon OHLCD Technology

Overhead Line Corrosion Detector (OHLCD) is industrialized by Teledyne Cormon in cooperation with CEGB research organization and is widely used by companies in the UK, France and Sweden. The detector encloses a winding and a pick-up coil and holds around the conductor. It can operate on any size ACSR dead line and also on live lines of up to 275kV. The manufacturer also claims that it can detect significant loss of aluminum cross section of up to 5% [10].

2) Fujikura's Detector

This technology was developed by Fujikura in cooperation with Tokyo Electric Power Company. In order for the implementation of inspection work, two methods: manpower inspection and auto inspection are offered. This detector has been embraced by numerous companies like Hokkaido Electric Power Company and Kyushu Electric Power Company [11].

3) Detection Services offered by ATTAR in Australia

Advanced Technology Testing and Research, (ATTAR), offers a NDT service for overhead line corrosion. It has more than 15 years of experience inspecting the condition of cables in the power industry. The device is positioned on live wires by a group of linesman and then operated remotely. It can be operated on lines with voltages over 500kV [12].

B. Time Domain Reflectometry

In comparison to other methods, TDR offers instinctive and simple analysis of the device under test. TDR is an electrical testing technique generally used to determine the location and condition of a device under test. It operates on the same principle as radar with the exception that the medium is a wire rather than air [13].

This method involves sending an electrical pulse (usually a short step) along a transmission line and observing the returning pulse energy on an oscilloscope [14], [15] as shown in Fig. 2.

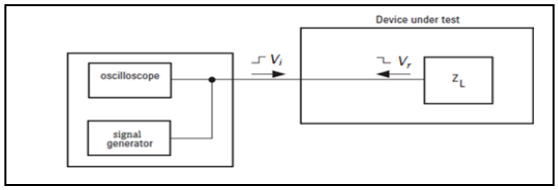

Figure 2. Block diagram of a time domain reflectometer

When the load impedance Z_L matches the characteristic impedance of the line Z_C no reflection occurs and the oscilloscope records the incident voltage step only, as seen in Fig. 3(a). However, when the travelling signal encounters any impedance change, part of the incident wave is reflected back. The reflected voltage wave then appears on oscilloscope in addition to the incident wave [14] as shown in Fig. 3(b).

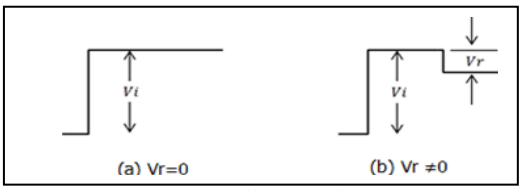

Figure 3. Oscilloscope displays [16]

The magnitude of the reflected signal can be calculated using reflection coefficient Γ, which is also in frequency domain, the ratio between reflected voltage wave V_r and the incident voltage wave V_i[15].

$$\Gamma = \frac{V_r}{V_i} = \frac{Z_L - Z_c}{Z_L + Z_c} \quad (10)$$

A transmission system terminated with an open circuit can be represented with a load of infinite impedance. In this case, there is no current passing through the load, while the voltage is at maximum. Therefore,

$$\Gamma = \frac{V_r}{V_i} = \frac{\infty - Z_c}{\infty + Z_c} = 1, \text{ or} \quad (11)$$

$$V_r = V_i \quad (12)$$

In case of an open circuit termination the reflected voltage ($Vr = Vi$) is added to the incident voltage. Fig. 4(a) shows the open circuit termination and its waveform.

On the other hand, a transmission system terminated with a short circuit can be represented with a load of zero impedance.

$$\Gamma = \frac{V_r}{V_i} = \frac{0 - Z_c}{0 + Z_c} = -1, \text{ or} \quad (13)$$

$$V_r = -V_i \quad (14)$$

In case of a short circuit termination the reflected voltage ($V_r = -V_i$) is added to the incident voltage. Fig. 4(b) shows the short circuit termination and its waveform.

Finally, a transmission system terminated with a matched impedance is represented with $Z_L = Z_C$. Therefore,

$$\Gamma = \frac{V_r}{V_i} = \frac{Z_C - Z_C}{Z_C + Z_C} = 0, \text{ or} \quad (15)$$

$$V_r = 0 \quad (16)$$

In case of matched impedance termination the reflected voltage ($V_r = 0$) is added to the incident voltage. Fig. 4(c) shows the short circuit termination and its waveform.

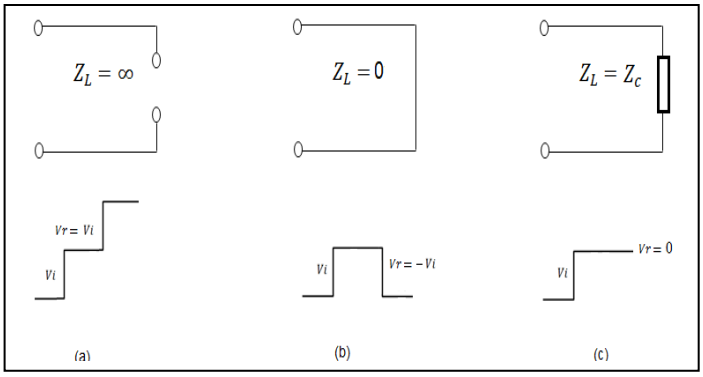

Figure 4. Typical load terminations and their respective waveforms

The velocity at which the signal moves down the line is measured in terms of phase constant β and the frequency of the signal. It is known as propagation velocity and is given by:

$$v_p = \frac{}{\beta} = \frac{2\pi f}{\beta} \quad (17)$$

$$v_p = \frac{}{\sqrt{LC}} = \frac{1}{\sqrt{LC}} \quad (18)$$

The reflected signal is easily distinguished as it is different in time from the initial signal. This time "t" is useful to find the distance d of the monitoring point to the mismatch.

$$d = v_p \frac{t}{2} \quad (19)$$

The characteristic impedance Z_C is given by [17]:

$$Zc = \sqrt{\frac{R+jL}{G+jC}} \quad (20)$$

In case of a lossless transmission line, the characteristic impedance of the line is approximated by:

$$Zc = \sqrt{\frac{L}{C}} \quad (21)$$

III. Application of TDR in this Project

A. Calibration of TDR Measuring System

The main objective of this paper is to detect and locate corrosion in ACSR cables of overhead transmission lines. For this purpose, an overhead transmission line consisting of ACSR conductor is randomly selected. The conductor is "Hare" obtained from [18] which has a 6:1 aluminum to steel strand ratio. The overall length "l" of this transmission line is assumed to be 250 km. Moreover, it is assumed that the conductor is corroded at different points along the length of the line.

The parameters of this transmission line are as follow:

$R = 0.33\ \Omega/\text{km}$; $L = 0.94\ \text{mH/km}$;

$C = 12.2\ \text{nF/km}$; $Zc = 277\Omega$

Using these values, the velocity of propagation is:

$$v_p = 2.95 \times 10^5 \text{km/s}. \quad (22)$$

And the propagation time for the pulse is:

$$t_p = \frac{l}{v} = 0.847\ \text{ms} \quad (23)$$

B. Modelling in SimPowerSystems Toolbox

In order to conduct TDR analysis, the circuit simulators SimPowerSystems [19] was chosen for modeling and simulating the system.

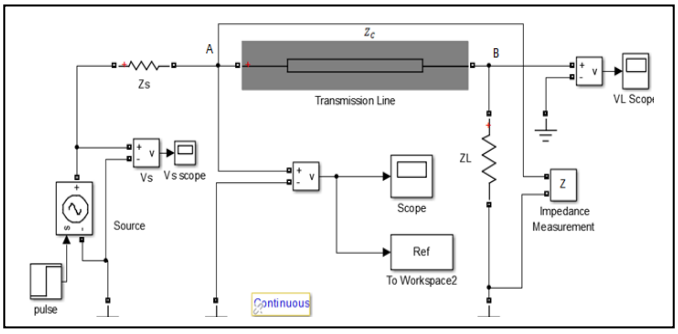

Figure 5. Block diagram for TDR analysis on transmission line

The basic block diagram for TDR analysis in SimPowerSystems is shown below in Fig. 5. In this block diagram, the transmission line is represented by a distributed parameter line model. The values of the system parameters comprising ACSR conductor "Hare" are entered in the corresponding parameter block of the distributed parameter line. A pulse of 20V amplitude is provided through the source with impedance $Z_s = 50\Omega$, while the load Z_L is being varied to simulate different terminations. Initially the incident voltage $V_i = V_s\left(\frac{Z_c}{Z_c+Z_s}\right)$, enters the line at point A. After a propagation delay of $t_p = 0.847\text{ms}$, the signal arrives unchanged at the other end of the line at point B. Part of this signal $V_r = \Gamma V_i$, is reflected back from the load. This reflected signal, in addition to the incident one is then measured at point A shown in Fig. 5.

IV. Simulation Results and Discussion

A. Detection and Localization of Corrosion

In order to detect corrosion at various points, the line is divided into segments of smaller length as seen in Fig. 6.

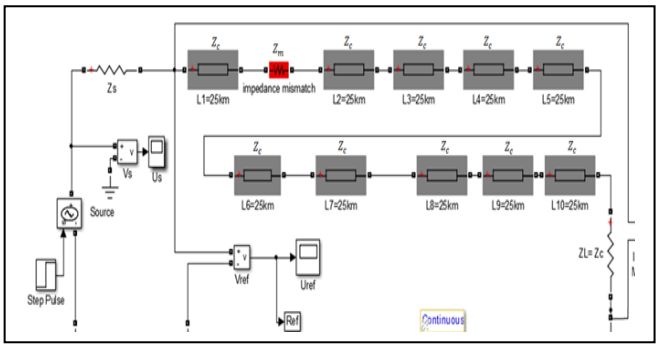

Figure 6. Corrosion planted at 25km on the line

At this stage in the circuit, a manipulated impedance mismatch representing corrosion in the cable is set at 25km from the source along the length of the line. The circuit was then simulated and the result is shown in Fig. 7.

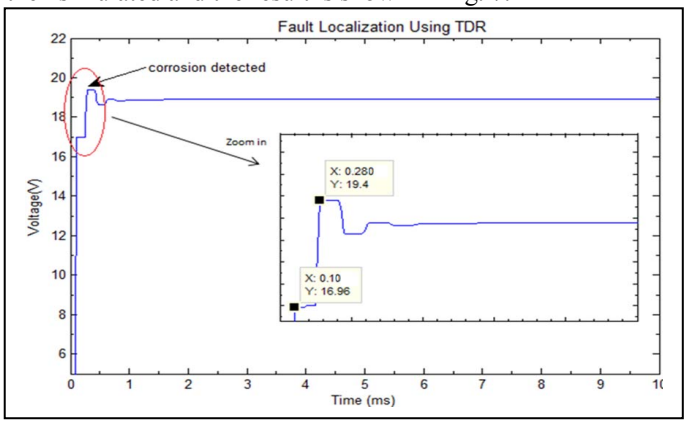

Figure 7. TDR Result for corrosion at 25 km

It can be seen that a reflection is detected due to the impedance mismatch. The step time of the pulse is 100μs while the detected reflection appears at 280μs. The time

difference between the two shows the time the wave has taken to travel to the point of the fault and back again to the measuring point, where it was detected. The location of this fault is then,

$$d = (2.95 \times 10^5)\left(\frac{0.28-0.1}{2} \times 10^{-3}\right) \quad (24)$$

$$d = 26.55 \text{ km} \quad (25)$$

Hence, the corrosion in the cable of the transmission line is detected and localized to be at 26.55km while the actual fault location was 25km, an error of 6.2%.

This process of simulation was then continued for three more samples where the impedance mismatch due to corrosion was set at 100km, 150km and 200km. The corresponding TDR results are summarised in Table II.

TABLE II. TDR RESULT FOR EACH SINGLE FAULT ON THE LINE

Actual Location (km)	Fault Time (s)	Measured Location (km)	Error (%)
25	2.8E-04	26.6	6.2
100	8.0E-04	103.3	3.3
150	1.15E-03	154.9	3.3
200	1.49E-03	205.0	2.5

B. Multiple Corrosions

The system under consideration was then tested for its capability to detect multiple corrosions. Fig. 8 represents block diagram of the system with corrosion planted at two locations, 25km and 75km. Two mismatched impedances Z_{m1} and Z_{m2}, each 50Ω, were used to represent them.

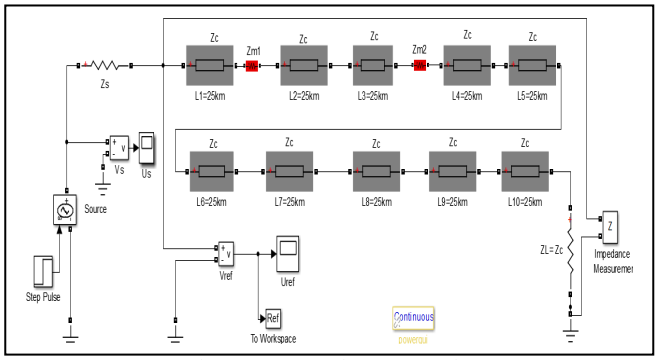

Figure 8. Corrosion at two points

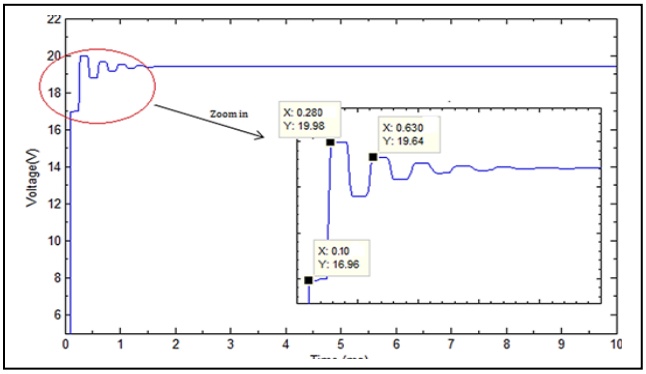

Figure 9. TDR Result for multiple corrosion at two points

In Fig. 9 the reflections at two points of time are shown. After the step time of 100µs of the incident pulse, the first reflection at 280µs indicates the corrosion due to the first impedance mismatch Z_{m1} at 25km. while the second reflection at 630µs is due to the impedance mismatch Z_{m2} at 75km.

TABLE III. TDR RESULT FOR TWO FAULTS ON THE LINE

Actual Location (km)	Step Time (s)	Fault Time (s)	Measured Location (km)	Error (%)
25	1.0E-04	2.8E-04	26.6	6.2
75	1.0E-04	6.3E-04	78.2	4.3

Table III shows that the faults at two different locations on the line are detected successfully. The number of mismatch impedances was then increased stepwise. For the line with fault at three points the results are summarised in Table IV.

TABLE IV. TDR RESULT FOR THREE FAULTS ON THE LINE

Actual Location (km)	Step Time (s)	Fault Time (s)	Measured Location (km)	Error (%)
25	1.0E-04	2.8E-04	26.6	6.2
75	1.0E-04	6.3E-04	78.2	4.3
200	1.0E-04	1.3E-03	181.4	9.3

Table IV shows that TDR analysis was able to estimate the location of corrosion at three points along the line. However, a combination of three mismatch impedances in this case led to an increase in the percentage error of up to 9.3%.

Finally, the number of mismatch impedances on the line was increased to five and the result is shown in Fig.10 below.

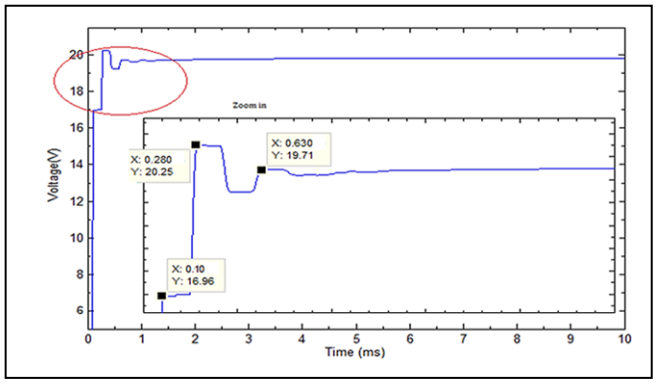

Figure 10. TDR Result for multiple corrosion at five points

The simulation of the circuit with combination of five mismatch impedances in this case results in detection of only two corroded points, i.e. at 25km and at 75km, while the other three faults are not localised. The interaction of multiple negative and positive waveforms ended up in cancellation of reflections and the circuit was unable to detect all the impedance mismatches. The results are summarised in Table V.

TABLE V. TDR RESULT FOR MULTIPLE CORROSION AT FIVE POINTS

Actual Location (km)	Step Time (s)	Fault Time (s)	Measured Location (km)	Error (%)
25	1.0E-04	2.8E-04	26.6	6.2
50	1.0E-04	undetected	undetected	N/A
75	1.0E-04	6.3E-04	78.2	4.3
175	1.0E-04	undetected	undetected	N/A
200	1.0E-04	undetected	undetected	N/A

V. CONCLUSION

In this paper, various techniques of corrosion detection in ACSR conductors of power transmission lines were discussed. The research showed that detectors based on electromagnetic induction technology can detect corrosion in steel strands as well as any flaw on aluminum strands. These detectors can identify flaws on a conductor well before other non-destructive tests could do. This method of corrosion detection is a promising technology and specialised in corrosion detection in ACSR conductors. Furthermore, the detectors not only operate on dead lines of any size but also on live lines of up to 500kV. The technology is highly sensitive, applicable, and feasible with ease of use compared to other technologies available. It has been used by companies around the globe successfully and is growing fast due to the high demand in power transmission industry.

The simulation outcome in TDR analysis proved that the circuit was able to detect and locate any single point corrosion along the line with an average error of less than 4%. When two mismatched impedances were placed in the circuit, the result showed successful detection and localisation of corrosion. When the circuit was modified for three mismatched impedances, the simulation graph still detected reflections for each location; however, this was done at the cost of increase in percentage error to 9.3%. Similarly, the circuit was modified to enclose five mismatches impedances. The results showed that the circuit was unable to display reflection for each corroded locations, while some reflections represented healthy locations on the line. This is concluded to be caused by multiple bouncing effect of the signal and the interaction of positive and negative reflections that ended up to cancel or even create the appearance of surplus reflections on the signal. Therefore, the existence of multiple corrosion on transmission lines causes degradation of measurement accuracy and hence decreases the capability of the technique to function properly and sufficiently.

REFERENCES

[1] A. V. Pinto, M. Z. Sebrao, C. R. S. H. Lourenco, I. S. de Almeida, J. Saad, and P. M. Lourenco, “Remote detection of internal corrosion in conductor cables of power transmission lines,” Paper read at Applied Robotics for the Power Industry (CARPI), 2010 1st International Conference on, 5-7 Oct. 2010.

[2] M. S. Mamiş, M. Arkan, and Cemal Keleş. (2013). "Transmission lines fault location using transient signal spectrum," International Journal of Electrical Power & Energy Systems no. 53 (0):714-718. [Online]. Available: http://dx.doi.org/10.1016/j.ijepes.2013.05.045.

[3] S. Karabay, and F. Kaya Önder. (2004). "An approach for analysis in refurbishment of existing conventional HV–ACSR transmission lines with AAAC," Electric Power Systems Research no. 72 (2):179-185. [Online]. Available: http://dx.doi.org/10.1016/j.epsr.2004.03.014

[4] J. Sutton, and K.G. Lewis, “The detection of internal corrosion in steel-reinforced aluminium overhead power line conductors,” in Proc. UK Corrosion, 1986, Birmingham, UK. Vol 1. Pp. 345-359.

[5] E. W. Greenfield, and E. W. Everhart, "A field ftudy of ACSR cable in severe sarine and industrial environment," Power Apparatus and Systems, Part iii. Transactions of the American Institute of Electrical engineers no. 76 (3):106-117. 1957.

[6] W. Liu, R. Hunsperger, M. Chajes, and E. Kunz, “An overview of corrosion damage detection in steel bridge strands using TDR,” Paper read at Proc., 2nd Int. Symp. on TDR for Innovative Applications, 2001.

[7] S. A. Fisher, I. R. Funnel, and S.T. Larsen, “The detection of overhead line conductor damage by helicopter borne thermal images,” Sixth International Symposium on High Voltage Engineering, New Orleans, 1989.

[8] J. Hansen, (2004, May). “The Eddy current inspection method, Part 1 – History and electrical theory,” Insight Vol 46 No. 5, pp 279 - 281.

[9] M. Komoda, T. Kawashima, M. Minemura, A. Mineyama, M. Aihara, Y. Ebinuma, T. Kanno, and M. Kiuchi, "Electromagnetic induction method for detecting and locating flaws on overhead transmission lines," Power Delivery, IEEE Transactions on no. 5 (3):1484-1490, Jul. 1990. [Online].Available: http://ieeexplore.ieee.org/stamp/stamp.jsp?tp=& arnumber=57992&isnumber=2105

[10] Cormon. A Teledyne Technologies Company. 2013. accessed on 10/10/2013, [Online]. Available: http://www.cormon.com/products/datasheets%5Cptp002.pdf

[11] Fujikura. Fujikura News, (Jul. 2012), accessed 11 02, 2013, [Online]. Available: http://www.fujikura.co.jp/ng/f-news/372.pdf

[12] Advanced Technology Testing and Research. ATTAR. 2013, accessed 11/05/2013, [Online]. Available:http://www.attar.com.au/overhead-line-corrosion-detection.aspx

[13] Y. H. Md. Thayoob, A. M. Ariffin, and S. Sulaiman, “Analysis of high frequency wave propagation characteristics in medium voltage XLPE cable model,” Paper read at Computer Applications and Industrial Electronics (ICCAIE), 2010 International Conference on, 5-8 Dec. 2010.

[14] S. Qinghai, U. Troeltzsch, and O. Kanoun, “Detection and localization of cable faults by time and frequency domain measurements,” Paper read at Systems Signals and Devices (SSD), 2010 7th International Multi-Conference on, 27-30 June 2010.

[15] G. M. Hashmi, R. Papazyan, and M. Lehtonen, “Comparing wave propagation characteristics of MV XLPE cable and covered-conductor overhead line using time domain reflectometry technique,” Paper read at Electrical Engineering, 2007. ICEE '07. International Conference on, 11-12 April 2007.

[16] Hewlett-Packard, (1998), “Time domain reflectometry theory,” Hewlett-Packard Application Note 1304-2, Hewlett-Packard Company, Palo Alto, Calif.

[17] H. Saadat, Power System Analysis. 2nd ed. Boston: McGraw-Hill. 2002.

[18] General Cable, (2013) Energy Cables ACSR, accessed on 28/09/2013 [Online].Available:http://www.generalcable.com.au/getattachment/7046493c-989c-418e-8735-ea3642d20082

[19] Mathworks, (2013), Accessed on: 01/11/2013 [Online]. Available: http://www.mathworks.com.au/products/simpower/